Elastic and inelastic scattering of K^+ from nuclei

A. A. Ebrahim and S. A. E. Khallaf
Physics Department, Assiut University, Assiut 71516, Egypt
(Received 28 May 2002; published 28 October 2002)

Local optical model calculations have been carried out for elastic, inelastic, total, and reaction cross sections of K^+ from ^{2}H, ^{6}Li, ^{12}C, and ^{40}Ca at kaon laboratory momenta ranging from 488 to 800 MeV/c. Zero-range distorted-wave Born approximation calculations have been carried out for elastic and inelastic scattering of K^+ leading to the lowest 3^+ state in ^{6}Li and 2^+ and 3^- states in ^{12}C. Local optical potential is also used to estimate quadrupole noncentral contributions to elastic K^+ scattering from the 1^+ ground state of ^{6}Li, and these are found to be very small. Deformation lengths extracted from inelastic scattering are similar to those deduced from other works. Our calculations adequately reproduced the kaon scattering data.

DOI: 10.1103/PhysRevC.66.044614 PACS number(s): 25.80.Nv, 24.10.Eq, 24.10.Ht

I. INTRODUCTION

Below 800 MeV/c, the K^+-nucleon (N) strong interaction has a minor energy and momentum dependence and is the weakest of all strong interaction processes. The typical K^+-N cross section (which is 10 mb on the average) is much smaller than π-N and K^--N cross sections in the same momentum region [1]. The implication for K^+-nucleus scattering is significant. The K^+ has a long mean free path in nuclear matter ($\lambda > 5$ fm) and is therefore capable of probing the interior of dense nuclei. This may be regarded as a result of the quark content of the K^+, which cannot annihilate with valence quarks of a nucleon. Isospin-average K^+-N amplitudes are determined mostly by the S11 phase shift at momenta below 800 MeV/c [2–4], and as a result, the K^+-nucleus interaction is highly elastic and dominated by single scattering.

The first studies of elastic scattering of K^+ from ^{12}C and ^{40}Ca gave cross sections larger than the predictions of optical model theories [5], and total cross sections for K^+ mesons on several nuclei at a range of kaon lab momenta also exceeded model expectations [6,7], as an indication that the nucleons within the nuclear medium do not behave as they do in free space. These observations led to several suggestions on how to remove the problem, including the interesting suggestion that medium modification such as nuclear swelling or meson mass scaling might be responsible for the lack of agreement with experimental data. Siegel *et al.* [7] proposed that the nuclear environment may modify the S11 K^+ scattering amplitude by altering the effective nucleon size in the nucleus. They found that an increase of 10–20 % in the S11 phase shift would markedly improve their agreement with data above 720 MeV/c. Such an increase is in line with the estimates of Close *et al.* [8] on the change of confinement scale in nuclei.

Recently, elastic and inelastic scattering of K^+ from ^{6}Li and ^{12}C at 635 and 715 MeV/c were analyzed [9], using the distorted wave impulse approximation (DWIA). The DOKAY code was used with several values of a scale factor f multiplied into both the real and imaginary amplitudes for each K^+-nucleon collision within a nucleus representing a medium enhancement factor for the K^+-N interaction [10]. A scaling factor near 20–30 % was needed to bring elastic and inelastic scattering of K^+ from ^{12}C into agreement with the experimental data. This was found to be true with K^+-^{6}Li elastic scattering [10], while for the inelastic scattering from ^{6}Li the scaling factor needed was $f = 1.0$. Generally, all the previous calculations of K^+-nucleus scattering, which were based on the impulse approximation, fall lower than the experimental data. On the other hand, in Ref. [11] the K^+ scattering sensitivity to the whole nuclear volume is maintainable. As a refinement on the PWIA the distorted wave Born approximation (DWBA) should be quantitatively accurate for K^+ reactions [11].

In the present work, the local potential of Johnson and Satchler [12] (equivalent to the Kisslinger nonlocal potential [13]) is used to analyze the differential elastic, inelastic, total, and reaction cross sections of K^+ from ^{2}H, ^{6}Li, ^{12}C, and ^{40}Ca at kaon Lab momenta ranging from 488 to 800 MeV/c. The DWUCK4 code [14] is used to calculate the angular distributions for the elastic and inelastic differential cross sections of the K^+ leading to the lowest 3^+ state in ^{6}Li at 715 MeV/c, 2^+ and 3^- states in ^{12}C at 635, 715, and 800 MeV/c, and elastic scattering differential cross sections from ^{40}Ca at 800 MeV/c.

Equivalent local potential of Johnson and Satchler is used with 10–15 % increasing in the S11 K^+-N phase shift to fit the available K^+ data [5,9] and then this potential is deformed to calculate the inelastic scattering angular distributions of K^+ from ^{6}Li and ^{12}C. The overall normalization of the calculated inelastic cross sections to data gives the deformation lengths which are considered here as free parameters in each case. The deformation lengths are extracted and compared to those predicted by others. Here, the deformation lengths are extracted by visually adjusting the calculations to the corresponding data.

The aim of the present work is to improve the agreement between measurements and calculations by increasing the S11 phase shift by about 10–15 %. A local optical potential analysis of the elastic scattering data on ^{6}Li, ^{12}C, and ^{40}Ca has been carried out. The local optical potentials obtained from this analysis have been used in a DWBA analysis of the inelastically scattered kaons to the first excited state (3^+; 2.186 MeV) in ^{6}Li and to the (2^+; 4.44 MeV) and (3^-; 9.64

MeV) states in ^{12}C. The method employed here is described in Sec. II, results and discussion are in Sec. III, and conclusions are in Sec. IV.

II. METHOD

Success of using the equivalent local potential of Johnson and Satchler [12] calculations for pions elastically and inelastically scattered from a variety of nuclei at different energies [15,16] motivated us to consider a similar method to the elastic and inelastic scattering of kaons from nuclei because of the great similarity between pions and kaons. Here, we have used the local pion-nucleus optical potential of Johnson and Satchler [12] that is exactly equivalent to the nonlocal potential of the Kisslinger form [13], with the necessary modifications required for the present case. The equivalent local potential can be obtained by using the Krell-Ericson transformation, which converts the relativistic Klein-Gordon equation for kaon scattering to the nonrelativistic Schrödinger equation. The DWUCK4 code which solves the nonrelativistic Schrödinger equation is employed in the present analysis, since the DWUCK4 program is widely available. This program was originally written to calculate the scattering and reaction observables for binary nuclear reactions using the DWBA [14].

The Coulomb potential considered here is due to the uniform charge distribution of the target nucleus of radius $R_C = r_C A^{1/3}$, where A is the target mass number and $r_C = 1.2$ fm ([16], and reference therein). The nuclear local transformed potential $U_{\rm loc}$ is [12]

$$U_{\rm loc}(r) = U_N(r) + \Delta U_C(r), \tag{1}$$

the nuclear part of the local potential $U_N(r)$ is [12]

$$U_N(r) = \frac{(\hbar c)^2}{2\omega}\left\{ \frac{q(r)}{1-\alpha(r)} - \frac{k^2\alpha(r)}{1-\alpha(r)} - \left[\frac{\frac{1}{2}\nabla^2\alpha(r)}{1-\alpha(r)} + \left(\frac{\frac{1}{2}\nabla\alpha(r)}{1-\alpha(r)} \right)^2 \right] \right\}, \tag{2}$$

and the Coulomb correction term $\Delta U_C(r)$ is [12]

$$\Delta U_C(r) = \frac{\alpha(r)V_C - (V_C^2/2\omega)}{1-\alpha(r)}, \tag{3}$$

where ω is the total energy of the kaon in the center of mass (c.m.) system. $q(r)$ and $\alpha(r)$ are complex and depend upon the separation distance between the kaon and the nucleus. The quantity $q(r)$ mainly results from the s-wave part and $\alpha(r)$ results from the p-wave part of the kaon-nucleon interaction. The functions $q(r)$ and $\alpha(r)$ are of short range and closely related to the nuclear matter distribution in the nucleus, both are energy dependent and given in detail in Ref. [12]. The kaon-nucleon scattering amplitude depends on complex first- and second-order interaction parameters. The first-order interaction parameters are related to the free kaon-nucleon scattering parameters through the phase shifts in the form described in Ref. [17] and the phase shifts are extracted from the SP92 solution of the phase shift compilation SAID code [18]. The first-order interaction parameters are then used to generate the complex local potential $U_{\rm loc}$ using the expressions from Ref. [12]. In this work, the second-order interaction parameters are neglected [19].

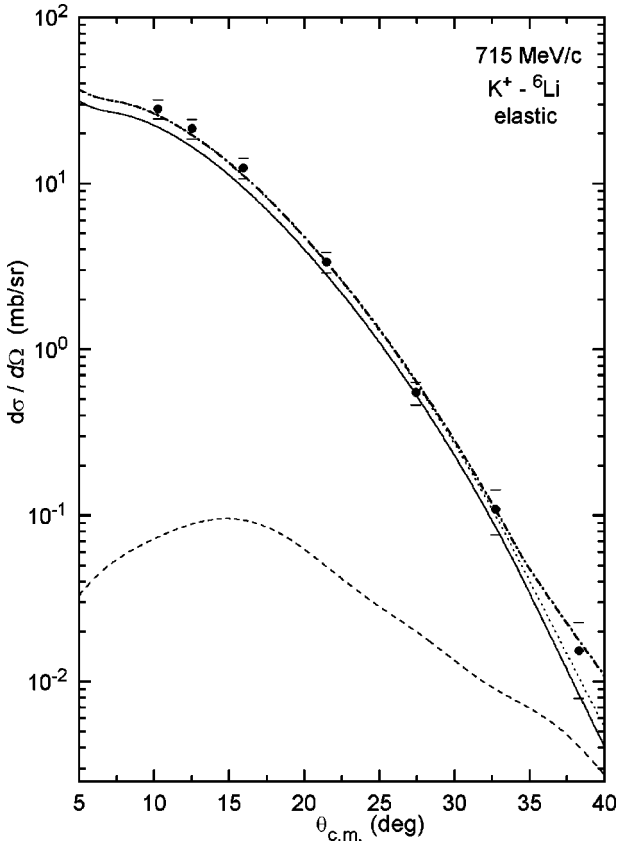

FIG. 1. Elastic scattering differential cross sections for 715 MeV/c K^+ on ^{6}Li. The solid curve is the central local potential predictions from the present work, the dotted curve is the same but with increasing the S11 K^+-N phase shift by 10%, the dashed curve shows the quadrupole elastic scattering with increasing S11 K^+-N phase shift by 10% calculated using the DWUCK4 code as described in the text, the dot-dashed curve shows the sum of dotted plus dashed curves, and the solid circles represent the experimental data taken from Ref. [9].

Calculations carried out by others [9,20] treat ^{6}Li as a 0^+ state, although the ground state of ^{6}Li has $J^P = 1^+$. The 1^+ ground state of ^{6}Li permits incoherent magnetic dipole and electric quadrupole scattering in addition to central, monopole scattering. Our calculations estimate the quadrupole corrections to the calculated elastic scattering differential cross section and compared to calculations that include only central scattering (see Fig. 1), as appropriate to spin zero target nuclei. The magnetic dipole scattering has been neglected because spin-flip scattering of K^+ mesons is weak at small angles [9]. The electric quadrupole contributions are important for angles greater than 25° [21], so these quadrupole contributions must be considered. We use the present first-order local potential to evaluate a part of the noncentral elastic scattering for ^{6}Li.

TABLE I. Kinematic factors for use in a nonrelativistic Schrödinger equation used in present work with kaon lab momentum $P_{\rm lab}$. E_L, M_k, k, and p_1 are the effective bombarding energy, effective kaon mass, kaon wave number, and kinematic transformation factor, respectively.

Target	$P_{\rm lab}$ (MeV/c)	E_L (MeV)	M_k (u)	$k(\mathrm{fm}^{-1})$	p_1
^{6}Li	715	318.23	0.85304	3.155	1.6224
^{12}C	635	260.54	0.82852	3.012	1.7105
	715	307.72	0.888776	3.368	1.7586
	800	358.41	0.95457	3.751	1.8106
^{40}Ca	800	346.34	0.99142	3.955	1.9433

Different formulas of the radial density distribution of nucleons for the considered nuclei in our calculations are used. The charge distribution of ^{6}Li was described in the form [22]

$$\rho_{\rm ch}(r)=\frac{Z}{8\pi^{3/2}}\left[\frac{1}{a^3}\exp\left(\frac{-r^2}{4a^2}\right)-\frac{c^2(6b^2-r^2)}{4b^7}\exp\left(\frac{-r^2}{4b^2}\right)\right], \tag{4}$$

with $a=0.928$ fm, $b=1.26$ fm, $c=0.48$ fm, and Z is the atomic number. Here, distributions of neutrons and protons within ^{6}Li nucleus are taken to be the same, since it is a light nucleus. We used the harmonic oscillator form for ^{2}H and ^{12}C nuclear densities:

$$\rho_m(r)=\rho_0\left[1+\alpha\left(\frac{r}{a}\right)^2\right]\exp\left(\frac{-r^2}{a^2}\right), \tag{5}$$

with parameters $\alpha=0.0$ and $a=1.71$ fm for ^{2}H [23] and $\alpha=2.234$ and $a=1.516$ fm for ^{12}C [9]. Also, we use the three parameter Fermi (3PF) shape distribution of nucleons for ^{40}Ca with parameters taken from Ref. [16] and references therein:

$$\rho_m(r)=\rho_0(1+\omega r^2/c^2)/\{1+\exp[(r-c)/a]\}, \tag{6}$$

ρ_0 can be evaluated from the normalization condition:

$$\int \rho_m(r),d\vec{r}=A. \tag{7}$$

The radial parts of the hadronic transition potential used here are as follows [24]:

$$V(r)=-\delta_l\frac{dU_{\rm loc}}{dr}, \tag{8}$$

where $U_{\rm loc}$ is the local transformed potential found to fit the corresponding elastic scattering data. For a given transition, we use δ_l to denote the corresponding real and imaginary ''deformation lengths'' for the K^+ interaction, while l ($=2$ or 3) is the multipolarity.

III. RESULTS AND DISCUSSION

We have used the first-order equivalent local optical potential with increasing the S11 K^+-N phase shift by about 10–15 % to analyze the elastic, inelastic, total, and reaction cross sections of positive kaons with lab momenta ranging from 488 to 800 MeV/c from ^{6}Li, ^{12}C, and ^{40}Ca nuclei. The first-order parameters are calculated using the increased S11 K^+-N phase shift and these parameters are then used to generate the corresponding real and imaginary parts of the optical potential. A 10–12 % change in the S11 phase shift yields improvements by about 15% for ^{6}Li and 15–20 % for ^{12}C and ^{40}Ca in the present elastic and inelastic differential cross sections. The resulting kinematic and parameter values for the cases studied here are calculated according to equations given in Ref. [24] and are listed in Table I. The present equivalent local potential when deformed and applied to inelastic scattering data for the excitation of 3^+ state in ^{6}Li and 2^+ and 3^- states in ^{12}C is able to reproduce the available experimental data [5,9]. In the present calculations we found that the Ericson-Ericson Lorentz-Lorentz (EELL) (a short-range correlation) parameter ζ slightly affects the elastic and inelastic scattering of K^+ differential cross sections. This parameter was found to play a significant role on the calculations of $\pi^\pm$ at the (3,3) resonance region where the diffraction minima move out with increasing ζ and the calculations involving $\zeta=1.0$ are much closer to the data than those with $\zeta=1.8$ [16]. Therefore, we have chosen $\zeta=1.0$ for use in the present calculations. Coulomb excitation was found to have a negligible effect. Also, it was noticed during this work specially for the case of ^{6}Li that no significant changes in the differential cross sections fit occur on raising r_C over 1.2 fm.

Figure 1 shows the present calculations of the differential elastic cross section of K^+ from ^{6}Li at 715 MeV/c compared to the recent data [9] using the central density given by Eq. (4) for nuclear matter distribution in ^{6}Li nucleus. The solid curve is the central local potential predictions for ($0^+\rightarrow 0^+$) from the present work, whereas the dotted curve is the same but with increasing the S11 K^+-N phase shift by 10%. The dashed curve corresponds to the calculated collective quadrupole elastic strength for ($1^+\rightarrow 1^+$) with an excitation energy of 0.1 MeV with increasing the S11 K^+-N phase shift by 10%, and the dot-dashed curve shows the sum of both dotted and dashed curves. The quadrupole scattering transition strength was estimated in the collective DWBA model in the same fashion as for inelastic scattering. The deformation β was determined from the ground state quadrupole moment of $-0.083\,e$ fm^2 [25] and the rotational model [26] to be 0.017. It is clear that the quadrupole cross section makes no significant difference with data [9], but it

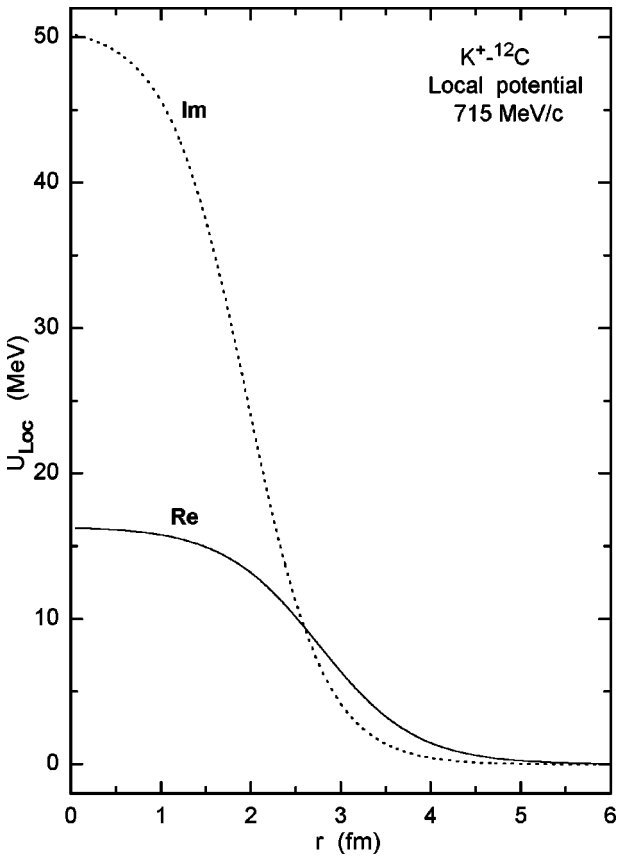

FIG. 2. Local optical potentials computed for 715 MeV/c K^+ scattered from ^{12}C with increasing the S11 K^+-N phase shift by 11%. The full curve is for the real potential and the dotted curve for the imaginary potential.

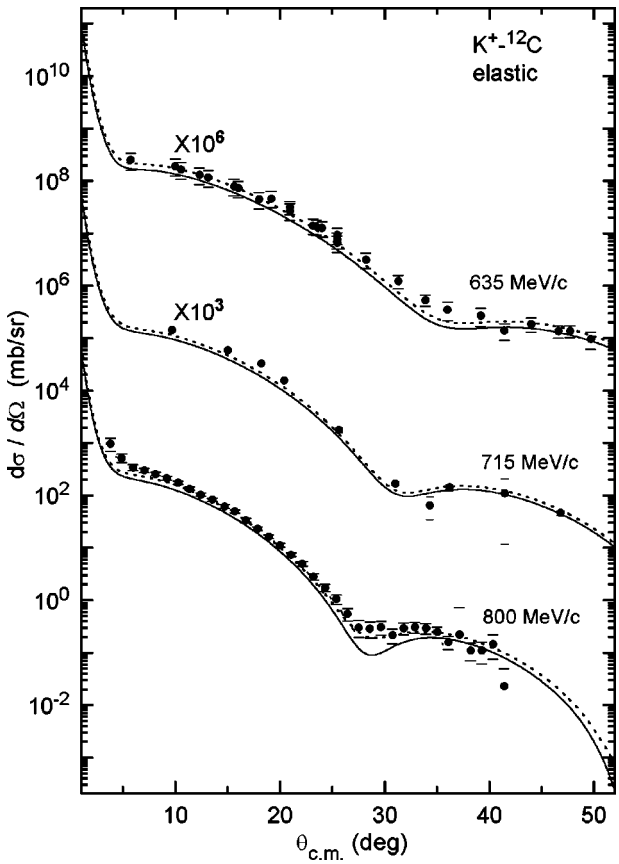

FIG. 3. Data for elastic scattering differential cross sections at momenta 635, 715, and 800 MeV/c K^+ from ^{12}C (Refs. [5,9]) compared to the local potential calculations. Calculations are shown without increase in S11 K^+-N phase shift by the solid curves, and the dashed curves show the same calculations but with increasing the S11 K^+-N phase shift by 11% for 635 and 715 MeV/c, and 12% for 800 MeV/c.

gives small contributions to monopole for ^{6}Li at angles greater than 30°.

The K^+-^{12}C complex local optical potential is shown in Fig. 2 at 715 MeV/c kaon laboratory momentum taking into account an increase of 11% in the S11 K^+-N phase shift. Both the real and imaginary parts are quite shallow and everywhere repulsive, with central strengths of about 17 and 50 MeV, respectively. The imaginary part is deeper and rapidly decreasing while the real part is shallower and wider. The radial shape of the real part Re(r) and the imaginary part Im(r) both follow the density $\rho(r)$. This behavior for both parts of the potential was observed for all cases under consideration. Previously, it was found that both real and imaginary potentials are repulsive for K^+-^{12}C at 300 MeV (Fig. 3.3 of Ref. [1]), while the real potential was repulsive and the imaginary potential was attractive for K^+-^{208}Pb at 200 and 500 MeV [11].

Differential elastic cross sections for K^+-^{12}C are shown in Fig. 3. No sharp diffraction minima are seen, neither in calculations nor in data. The comparison between our calculations and data [5,9] at 635, 715, and 800 MeV/c is shown in Fig. 3. The disagreement between our results and data is about 15% at 800 MeV/c but appears to decrease with decreasing momenta. We have a good agreement between data and the present calculations with increasing the S11 K^+-N phase shift by 12% at 800 MeV/c and 11% at 635 or 715 MeV/c.

In Fig. 4 we show the differential elastic cross sections data [5] of K^+ from ^{40}Ca at 800 MeV/c, compared to the present local optical potential predictions. A good agreement between the present calculations using the 3PF distribution for the ^{40}Ca density and $\zeta = 1.0$ is obtained with increasing the S11 phase shift by 12%. This modification in the phase shift gives cross sections higher by about 18% than the calculations using the local optical potential without increase of S11 K^+-N phase shift.

It is obvious that the K^+ elastic calculations using the first-order local potential need enhancement in the S11 K^+-N phase shift by about 10–12 % to have adequately agreement with data. This enhancement in the S11 phase shift can be related to nucleon size variation of a size consistent with current theoretical estimates which may indicate that the internal structure of a nucleon is appreciably altered by its surrounding nuclear environment.

Since inelastic scattering in the collective model is driven by the first derivative of the optical potential, agreement with such data can be a possible means to remove the ambiguity from elastic scattering fits. Angular distributions data [5,9]

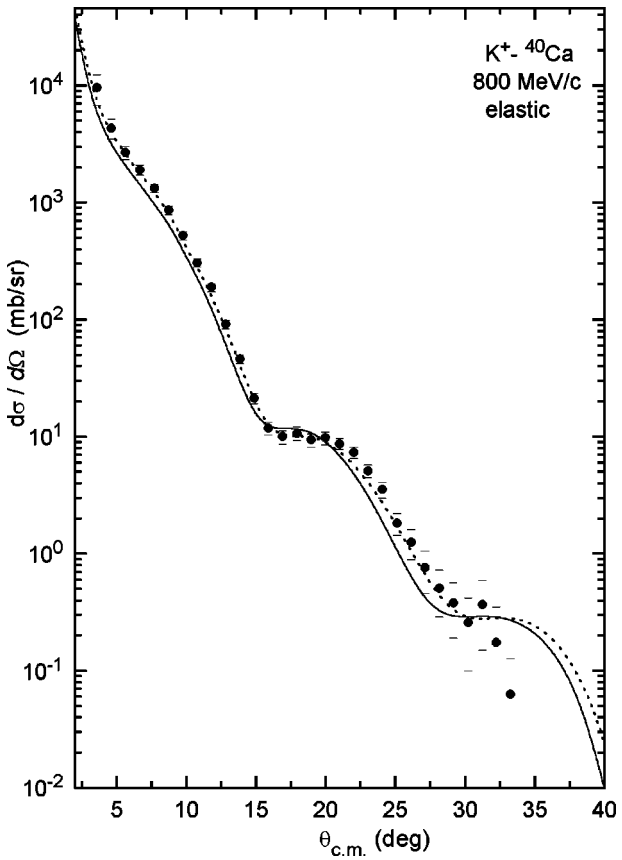

FIG. 4. As in Fig. 3, but for K^+-^{40}C elastic scattering differential cross sections at 800 MeV/c. The increase in S11 K^+-N phase shift used is 12%. The experimental data are taken from Ref. [5].

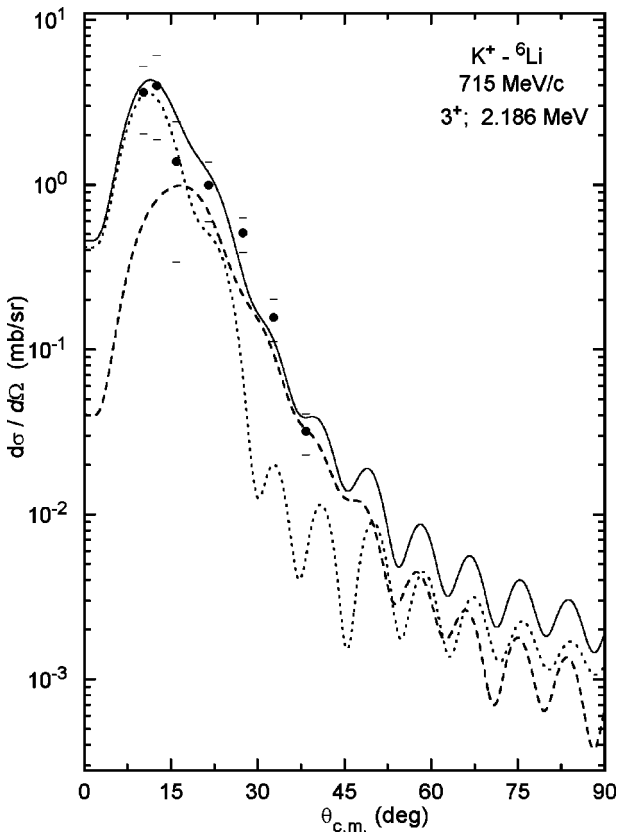

FIG. 5. Inelastic scattering differential cross sections at 715 MeV/c K^+ exciting the 2.186 MeV 3^+ state of ^{6}Li. Dotted and dashed curves correspond to $l=2$ and 4, respectively, and the solid curve is the sum of both them. All curves are with increasing S11 K^+-N phase shift by 10%. The experimental data are taken from Ref. [9].

for the inelastic scattering of kaons leading to the lowest 3^+ state in ^{6}Li and the lowest 2^+ and 3^- states in ^{12}C were computed by the DWBA method using the zero-range code DWUCK4 due to Kunz [14]. The extent of applicability of the conventional DWBA method with the local optical potential may be tested to predict observables of K^+ inelastically scattered from nuclei. Success is expected because of the close relation between elastic and inelastic scattering to collective states [24].

A collective model DWBA prediction using the equivalent local optical potential adequately fits the shape and magnitude of 715 MeV/c K^+ leading to the lowest 3^+ state in ^{6}Li and 635, 715, and 800 MeV/c to 2^+ and 3^- states in ^{12}C as shown in Figs. 5–7, with increasing the S11 K^+-N phase shifts by 10–12 % for both nuclei. In the analysis presented here, the deformation lengths are varied until agreement is obtained with K^+ data.

Figure 5 compares the values for the differential cross sections predicted from the present local potential calculations to the available K^+-^{6}Li inelastic data [9] at 715 MeV/c. To calculate the angular distributions of K^+ inelastically scattered to the first excited state (3^+; 2.186 MeV) in ^{6}Li, the allowed angular momentum transfers are determined according to the selection rules given by [27]

$$|J_i - J_f| \leq l \leq J_i + J_f, \quad \pi_i \pi_f = (-1)^l,$$

where J_i and J_f are the total angular momenta of the initial and final states, respectively. π_i and π_f are the initial and final parities. In the case under consideration $l=2$ or 4. Dotted and dashed curves in Fig. 5 correspond to $l=2$ and 4, respectively, and the solid curve is the sum of both of them. We use the same deformation lengths for both $l=2$ and 4 predictions in case of the real or imaginary local optical potential; our point is to have a good fit between data [9] and the sum of dashed and dotted curves, i.e., the solid curve. The extracted deformation lengths are listed in Table II. All curves shown in Fig. 5 correspond to an increase in the S11 phase shift by 10%. The narrow angular range of the available data emphasizes the need for further measurements of K^+-^{6}Li scattering.

Since the low-lying states in ^{12}C are known to be collective in nature, having negligible spin-flip contribution in the transition from the ground state [28], we considered the 4.44 MeV 2^+ and 9.64 MeV 3^- transitions. The available data for kaon inelastic scattering to these states are shown in Figs. 6 and 7.

Figures 6 and 7 display the predictions of the differential inelastic scattering cross sections of K^+ from ^{12}C nucleus excited to the lowest 2^+ and 3^- states at 635, 715, and 800 MeV/c. The inelastic data [5,9] are well represented by

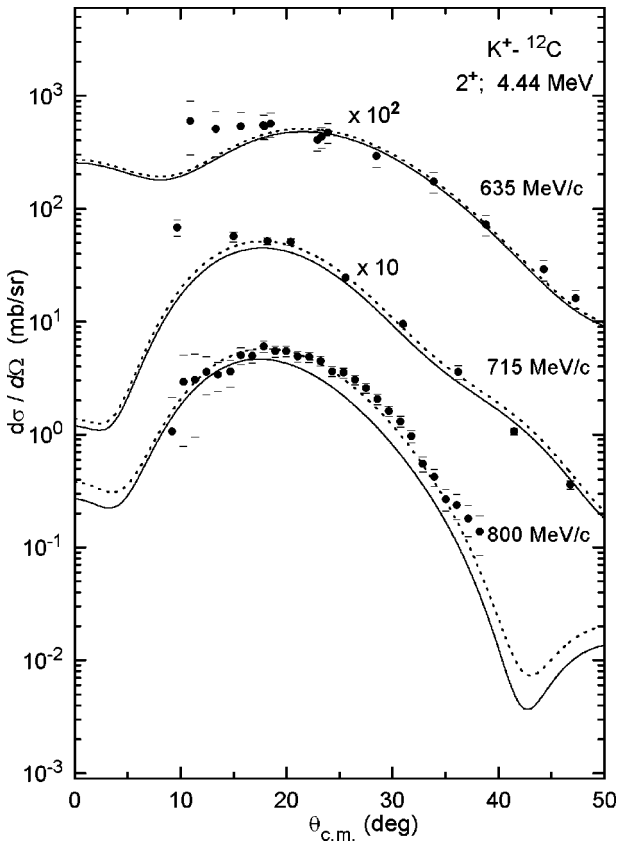

FIG. 6. As in Fig. 3, but for inelastic scattering differential cross sections for 635, 715, and 800 MeV/c K^+, Refs. [5,9], exciting the 4.44 MeV 2^+ state of ^{12}C.

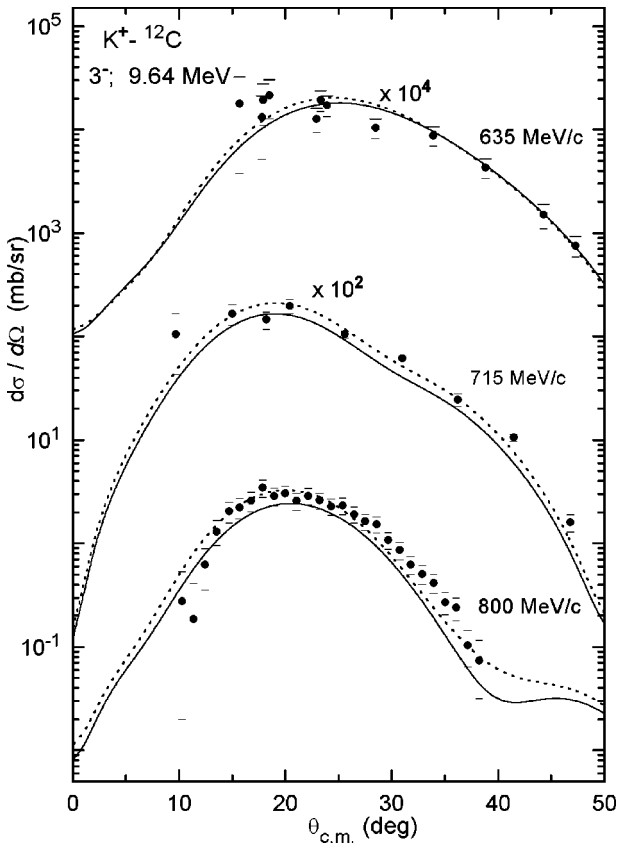

FIG. 7. As in Fig. 6, but for K^+ exciting the 9.64 MeV 3^- state of ^{12}C.

the present calculations by increasing the S11 phase shifts by about 11% for 635 and 715 MeV/c and 12% for 800 MeV/c.

The values of the deformation lengths for all collective states analyzed here are summarized in Table II. It can be seen from Table II that the values of imaginary deformation lengths determined here using the equivalent local optical potential for 2^+ and 3^- excited states in ^{12}C decrease with increasing kaon laboratory momenta. It is clear from Table II that the deformation lengths of the real potential are greater than the corresponding ones for the imaginary potential in all cases under consideration. Since the deformation lengths are more significant than deformation parameters [30] and when comparing excitations induced by different projectiles, it is more appropriate to compare deformation lengths rather than deformation parameters [31]. Table II shows the extracted deformation lengths from the present work and the corresponding ones previously extracted by others [32]. For the ^{12}C target, it is clear that δ_l ($l=2$ or 3) of the present work agrees reasonably with δ_l ($l=2$ or 3) given in Table II of Ref. [32] which ranges from 1.97 to 1.12 fm for the 2^+ state and from 1.25 to 0.65 fm for the 3^- state for different reactions at various energies. Moreover, δ_{real} for the (2^+; 4.44

TABLE II. Deformation lengths from K^+ inelastically scattered from ^{6}Li and ^{12}C compared to those predicted by others.

P_{lab}	Target	State	Present		Others			
(MeV/c)			δ_{real} (fm)	$\delta_{\text{imag.}}$ (fm)	δ (fm)	Reaction	Energy range (MeV)	Reference
635	^{12}C	2^+	1.725	1.114	1.12–1.97	p-^{12}C	40.0–168.0	[32]
715			1.355	1.005		d-^{12}C		
800			1.413	0.978		^{3}He-^{12}C		
635		3^-	1.512	1.214	0.65–1.23	α-^{12}C		
715			1.302	1.205		^{12}C-^{12}C		
800			1.319	0.955		^{16}O-^{12}C		
715	^{6}Li	3^+	1.923	1.522	2.0–3.0	^{6}Li-^{9}Be	7.0–12.0	[37]

TABLE III. Reaction and total cross sections (in mb) for the K^+ interaction with various nuclei calculated at various lab kaon momenta (in MeV/c) in the present work.

	σ_R			$\sigma_{\rm tot}$			
$P_{\rm lab}$	^{6}Li	^{12}C	^{40}Ca	^{2}H	^{6}Li	^{12}C	^{40}Ca
488	68.17	127.34	365.51	26.99	79.88	168.22	499.37
531	73.14	134.42	377.34	28.62	83.87	170.39	516.18
635	76.23	138.55	385.24	28.71	84.14	173.15	535.25
656	78.21	146.72	411.48	28.99	90.19	178.15	538.13
714	79.92	149.27	412.34	29.26	92.11	180.36	540.45
715	80.15	151.31	414.13	29.28	94.17	181.49	540.57
800	86.66	164.47	436.26	30.34	95.23	186.21	549.32

MeV) state ^{12}C given in Table II for the present work falls adequately close to the corresponding δ from different reactions, given in Refs. [31,33–35]. For ^{6}Li, the extracted $\delta_{\rm real}$ for the (3^+; 2.186 MeV) state given in Table II is very close to the deformation length given in Table III of Ref. [37], namely $\delta^{1^+\to 3^+}=2.0$ fm predicted from the ^{6}Li-^{9}Be reaction at $E_{\rm c.m.}=12$ MeV.

The DWUCK4 code using the present first-order local optical potential calculates the reaction cross sections σ_R of kaon scattering on ^{2}H, ^{6}Li, ^{12}C, and ^{40}Ca at kaon laboratory momenta ranging from 488 to 800 MeV/c. Following the same procedure, the total cross section $\sigma_{\rm tot}$ is calculated here as well according to the very well known relation [36]:

$$\sigma_{\rm tot}=\frac{2\pi}{k^2}\sum_L (2L+1)[1-{\rm Re}\,\eta_L], \tag{9}$$

where k is the incoming kaon's wave number and η_L is the projectile-nucleus non-Coulomb amplitude. The results of the present calculations with increasing the S11 phase shift by 12% for ^{6}Li and 15% for ^{12}C and ^{40}Ca are collected in Table III. In the present work, the calculation uses unaltered phase shifts for the K^+-deuteron calculation appropriate to its highly diffuse structure [7]. It can be seen from Table III that the total and reaction cross sections for the light nuclei increase with momentum, while for calcium there is only a weak momentum dependence. It is also noticed that $\sigma_{\rm tot}$ and σ_R increase as the mass number of target nucleus increases. Low values of $\sigma_{\rm tot}$ shown in Table III compared to the corresponding values for pion scattering [15,36] indicate a longer mean free path for K^+.

The possible changes of the K^+-N interaction in the nucleus can be calculated by the ratio [7]:

$$R_T=\frac{\sigma_{\rm tot}(K^+\text{-nucleus})/A}{\sigma_{\rm tot}(K^+\text{-deuteron})/2}. \tag{10}$$

The per nucleon total cross section ratios of nucleus to deuteron are calculated using the values of $\sigma_{\rm tot}$ in Table III and listed in Table IV. These ratios are all near unity; this reveals the near-linearity of the total cross section with mass number A. This suggests that the low-momentum K^+ is a good hadronic probe capable of penetrating a large part of the nuclear volume. In order to obtain agreement with the experimental data, we needed to enhance the S11 K^+-N phase shifts in ^{6}Li, ^{12}C, and ^{40}Ca but not in deuteron, as was done for the values in Table III. Low values of the reaction cross sections σ_R given in Table III confirm that positive kaons are weakly absorbed in nuclear matter.

IV. CONCLUSION

The angular distributions of the elastic scattering cross sections of K^+ on ^{6}Li, ^{12}C, and ^{40}Ca at 635, 715, and 800 MeV/c kaon laboratory momenta are analyzed using the DWBA with DWUCK4 code. The local optical potential needs

TABLE IV. The per nucleon total cross section ratios from the present work compared to those of Ref. [29].

	Present			From Ref. [29]		
$P_{\rm lab}$	$\frac{\rm Li/6}{\rm H/2}$	$\frac{\rm C/12}{\rm H/2}$	$\frac{\rm Ca/40}{\rm H/2}$	$\frac{\rm Li/6}{\rm H/2}$	$\frac{\rm C/12}{\rm H/2}$	$\frac{\rm Ca/40}{\rm H/2}$
488	0.986	1.039	0.925	1.016	1.090	1.039
531	0.977	0.992	0.902	0.979	1.038	0.983
635	0.977	1.005	0.932	—	—	—
656	1.037	1.025	0.928	1.015	1.043	0.947
714	1.049	1.027	0.923	1.013	1.039	0.932
715	1.072	1.033	0.923	—	—	—
800	1.046	1.023	0.905	—	—	—

an enhancement in the dominated S11 K^+-N phase shifts by 10% for low-density ^{6}Li, but 11–12 % were required for ^{12}C and ^{40}Ca nuclei. If the K^+-N phase shifts increase the nucleon size will increase; a ''swelling'' of the nucleon in nuclear medium. This means that the K^+-N interaction inside a nucleus will differ from the free space.

The local optical potential is also used to estimate quadrupole noncentral contributions to elastic K^+ scattering from the 1^+ ground state of ^{6}Li; these make no difference to data, but only gave small contributions to monopole for ^{6}Li at large angles. So, the 1^+ spin of ^{6}Li can be ignored, and we can treat the data in the same way as we did for zero-spin ^{12}C and ^{40}Ca nuclei. It is clear that the K^+ data and the present elastic calculations show a much less distinct diffraction pattern than is seen for the strongly absorbed pions. This is expected for scattering from a repulsive potential. The need for further measurements of K^+-^{6}Li scattering is stressed.

The differential inelastic scattering of K^+ to the first 3^+ state in ^{6}Li and lowest 2^+ and 3^- states in ^{12}C are calculated by the present local potential, and this potential has the ability of reproducing the shape and magnitude of the K^+ scattering data by the present calculations. The same enhancement in the S11 K^+-N phase shift is required for both elastic and inelastic scattering of K^+ at a certain energy from ^{6}Li or ^{12}C nuclei, while it is larger for $\sigma_{\rm tot}$ and σ_R in the case of ^{6}Li, ^{12}C, and ^{40}Ca. In general, these modifications in S11 K^+-N phase shifts bring all calculations for differential elastic, inelastic, total, and reaction cross sections and per nucleon total ratios more in line with the experimental data.

Finally, we conclude that our results from the present work based on the DWBA and also suggestions about nucleon swelling [10], with calculations based on the impulse approximation, as well as pion excess in nuclei [38,39], show the possibility of observing some unusual phenomena in the K^+-nucleus interaction. But the investigation of the in-medium effects in the theory of nuclear reactions is still in its early stages and needs more time to clarify and isolate exactly the role played by the nuclear medium in relevance to phenomena as described above. But we can adopt the ability of the present method to account for elastic and inelastic kaon data, demonstrating that local optical potential can serve as a reliable model for kaon-nucleus scattering.

[1] C.B. Dover and G.E. Walker, Phys. Rep. **89**, 1 (1982).
[2] B.R. Martin, Nucl. Phys. **B94**, 413 (1975).
[3] R.A. Arndt, L.D. Roper, and P.H. Steinberg, Phys. Rev. D **18**, 3278 (1978); A. Arndt and L.D. Roper, *ibid.* **31**, 2230 (1985).
[4] K. Hashimoto, Phys. Rev. C **29**, 1377 (1984).
[5] D. Marlow *et al.*, Phys. Rev. C **25**, 2619 (1982).
[6] M.F. Jiang, D.J. Ernst, and C.M. Chen, Phys. Rev. C **51**, 857 (1995).
[7] P.B. Siegel, W.B. Kaufmann, and W.R. Gibbs, Phys. Rev. C **31**, 2184 (1985).
[8] F.E. Close, R.L. Jaffe, R.G. Roberts, and G.G. Ross, Phys. Rev. D **31**, 1004 (1985).
[9] R.E. Chrien, R. Sawafta, R.J. Peterson, R.A. Michael, and E.V. Hungerford, Nucl. Phys. **A625**, 251 (1997).
[10] R.J. Peterson, A.A. Ebrahim, and H.C. Bhang, Nucl. Phys. **A625**, 261 (1997).
[11] C.B. Dover and P.J. Moffa, Phys. Rev. C **16**, 1087 (1977).
[12] M.B. Johnson and G.R. Satchler, Ann. Phys. (N.Y.) **248**, 134 (1996).
[13] L.S. Kisslinger, Phys. Rev. **98**, 761 (1955).
[14] P. D. Kunz, computer code DWUCK4, University of Colorado; P. D. Kunz and E. Rost, in *Nuclear Reactions*, Vol. 2 of *Computational Nuclear Physics*, edited by K. Langanke, J. A. Maruhn, and S. E. Koonin (Springer-Verlag, New York, 1993).
[15] S.A.E. Khallaf and A.A. Ebrahim, Phys. Rev. C **65**, 064605 (2002).
[16] S.A.E. Khallaf and A.A. Ebrahim, Phys. Rev. C **62**, 024603 (2000).
[17] J. Bartel, M.B. Johnson, and M.K. Singham, Ann. Phys. (N.Y.) **196**, 89 (1989); S.J. Greene *et al.*, Phys. Rev. C **30**, 2003 (1984); R. A. Gilman, Ph.D. dissertation, University of Pennsylvania (1985).
[18] R.A. Arndt and L.D. Roper, Phys. Rev. D **31**, 2230 (1985); Phys. Rev. E **46**, 961 (1992).
[19] O. Meirav, E. Friedman, R.R. Johnson, R. Olszewski, and P. Weber, Phys. Rev. C **40**, 843 (1989).
[20] R. Michael *et al.*, Phys. Lett. B **382**, 29 (1996).
[21] Elisabeth Romotsky and P.B. Siegel, Phys. Rev. C **57**, 1536 (1998).
[22] R.R. Kiziah *et al.*, Phys. Rev. C **30**, 1643 (1984); G.R. Satchler and W.G. Love, Phys. Rep. **55**, 183 (1979).
[23] W.W. Buck, J.W. Norbury, L.W. Townsend, and J.W. Wilson, Phys. Rev. C **33**, 234 (1986).
[24] G.R. Satchler, Nucl. Phys. **A540**, 533 (1992).
[25] F. Ajzenberg-Selove, Nucl. Phys. **A490**, 1 (1988).
[26] M. A. Preston, *Physics of the Nucleus* (Addison Wesley, Reading, MA, 1962), p. 66.
[27] R.H. Bassel, G.R. Satchler, G.R. Drisko, and E. Rost, Phys. Rev. **128**, 2693 (1962).
[28] W.B. Cottingame *et al.*, Phys. Rev. C **36**, 230 (1987).
[29] R. Weiss *et al.*, Phys. Rev. C **49**, 2569 (1994).
[30] G. R. Satcler, *Direct Nuclear Reactions* (Clarendon Press, Oxford, 1983), p. 619.
[31] A. Nadasen, M. McMaster, M. Fingal, J. Tavormia, J.S. Winfield, R.M. Ronningen, P. Schwandt, F.D. Bechetti, J.W. Jöneche, and R.E. Warner, Phys. Rev. C **40**, 1237 (1989).
[32] S.M. Smith, G. Tibell, A.A. Cowley, D.A. Goldberg, H.G. Pugh, W. Reichart, and N.S. Wall, Nucl. Phys. **A207**, 273 (1973), and references therein.
[33] A.F. Zeller, K.W. Kemper, D.C. Weisser, T.R. Ophel, D.F. Hebbard, and A. Johnston, Nucl. Phys. **A323**, 477 (1979).
[34] Y. Yasue, T. Tanabe, F. Soga, J. Kokame, F. Shimokoshi, J. Kasagi, Y. Katota, T. Ohsawa, and K. Furuno, Nucl. Phys. **A394**, 29 (1983).

[35] P.J. Moffa, C.B. Dover, and J.P. Vary, Phys. Rev. C **16**, 1857 (1977).
[36] A. Saunders, S. Høibråten, J.J. Kraushaar, B.J. Kriss, R.J. Peterson, R.A. Ristinen, J.T. Brack, G. Hofman, E.F. Gibson, and C.L. Morris, Phys. Rev. C **53**, 1745 (1996).
[37] E. Muskat, J. Carter, R.W. Fearich, and V. Hnizd, Nucl. Phys. **A581**, 42 (1995).
[38] M.F. Jiang and Daniel Koltun, Phys. Rev. C **46**, 2462 (1992).
[39] S.V. Akulinichev, Phys. Rev. Lett. **68**, 290 (1992).